

MHD simulations of jet formation - protostellar jets & applications to AGN jets

Christian Fendt, Bhargav Vaidya,
Oliver Porth and Somayeh Sheikh Nezami†

Max Planck Institute for Astronomy, Königstuhl 17, D-69117 Heidelberg, Germany
email: fendt@mpia.de

Abstract. Jet formation MHD simulations are presented considering a variety of model setups. The first approach investigates the interrelation between the disk magnetisation profile and jet collimation. Our results suggest (and quantify) that outflows launched from a very concentrated region at the inner disk tend to be weakly collimated. In the second approach, jet formation is investigated from a magnetic field configuration consisting of a stellar dipole superposed by a strong disk field. We find that the central dipole considerably de-collimates the disk wind. In addition, reconnection flares are launched in the interaction region of disk and stellar magnetic field, subsequently changing the outflow mass flux by factors of two. The time interval between flare ejection is about 1000 Keplerian periods - surprisingly similar to the observed time lag between jet knots. The third approach considers radiative pressure effects on jet collimation - an environment which is interesting mainly for outflows from massive young stars (but also for relativistic jets). Finally we present relativistic MHD simulations of jet formation from accretion disks extending the previous non-relativistic approaches.

Keywords. accretion, accretion disks, stars: magnetic fields, stars: mass loss, stars: winds, outflows, ISM: Herbig-Haro objects, galaxies: jets

1. Introduction

Highly collimated outflows are one of the most striking signatures of young stars. Jets are observed, however, also in other sources – among them micro-quasars or X-ray binaries (MQs, XRBs), or active galactic nuclei (AGN). In stellar sources, a central stellar magnetic field is surrounded by a disk carrying its own magnetic flux. Such a geometrical setup can be found young stars, cataclysmic variables, high-mass and low-mass X-ray binaries, and other micro-quasar systems. The current understanding of jet formation is that outflows are launched by *magnetohydrodynamic* (MHD) processes in the close vicinity of the central object – an accretion disk surrounding a protostar or a compact object Blandford & Payne (1982), Pudritz *et al.* (2007), Shang *et al.* (2007). The details of the physical processes involved are, however, not completely understood.

Jet formation simulations can be distinguished in those taking into account the evolution of the disk structure and others considering the disk surface as a fixed-in-time boundary condition for the jet (see below). The case of superposed stellar/disk magnetic fields is rarely treated in simulations, although the first models were discussed by Uchida & Low (1981). Simulations of a dipole with aligned vertical disk field were presented first by Hayashi *et al.* (1996), Hirose *et al.* (1997), or Miller & Stone (1997). The stellar magnetosphere impacts jet formation by enhancing the magnetic flux available, imposing a central pressure, or providing excess angular momentum in the launching area.

† Home institute: Ferdowsi University of Mashhad, Iran

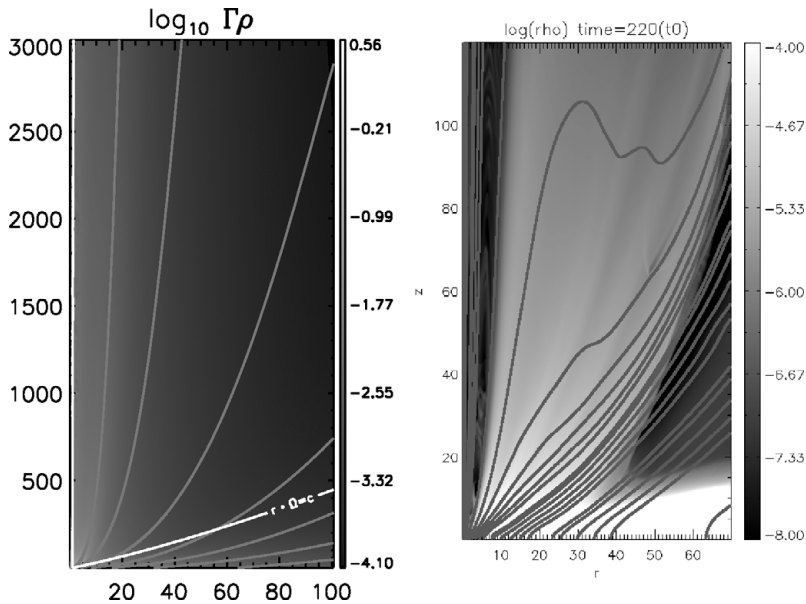


Figure 1. Jet formation simulations considering the disk as fixed-in-time boundary condition (left) and evolving the disk structure together with the outflow (right). The left figure shows a relativistic MHD simulation of jet formation by Porth & Fendt (2010) reaching Lorentz factors of about $\Gamma = 10$ (grid size 100x3000 inner disk radii). The outflow in the right figure originates in a $(h/r) = 0.1$ disk with density contrast 10^4 to the initial corona and disk resistivity $\eta = 0.01$ (grid size 812x1500 cells, resp. 80x120 inner disk radii).

Jet formation in massive young stars is a rather new topic. The conditions for jet launching as well as important jet parameters such as mass fluxes, velocities, or magnetic field strengths are hardly known. However, we know that massive stars have a strong radiation field which is expected to affect accretion as well as outflow processes.

2. Jet formation - the standard MHD model

The principal processes involved in jet formation can be summarized as follows.

(i) Magnetic flux is provided by the star-disk (or black-hole - disk) system - possibly by a disk or stellar dynamo, or by advection of the interstellar field. The star-disk system also drives an electric current.

(ii) Accreting material is diverted and launched as a plasma wind (from the stellar or disk surface), couples to the magnetic field, and is flung out magneto-centrifugally.

(iii) Inertial forces wind up the poloidal field inducing a toroidal component.

(iv) The plasma becomes accelerated magnetically (conversion of Poynting flux).

(v) The toroidal field tension collimates the outflow into a high speed jet beam.

(vi) The plasma velocities subsequently exceed the speed of the magnetosonic waves. The super-fast magnetosonic regime is causally decoupled from the surrounding medium.

(vii) Where the outflow meets the ISM, a shock develops, thermalizing the jet energy.

(viii) The underlying hypothesis is that jets can only be formed in a system with a high degree of axi-symmetry. This might be the reason why only few jets are found in cataclysmic variables or pulsars (e.g. see Fendt & Zinnecker (1998)).

The model of a dipole-plus-disk magnetic flux configuration were introduced for protostellar jets by Uchida & Low (1981). MHD simulations of jets from dipolar magnetospheres were performed by Uchida & Shibata (1984), Uchida & Shibata (1985). However,

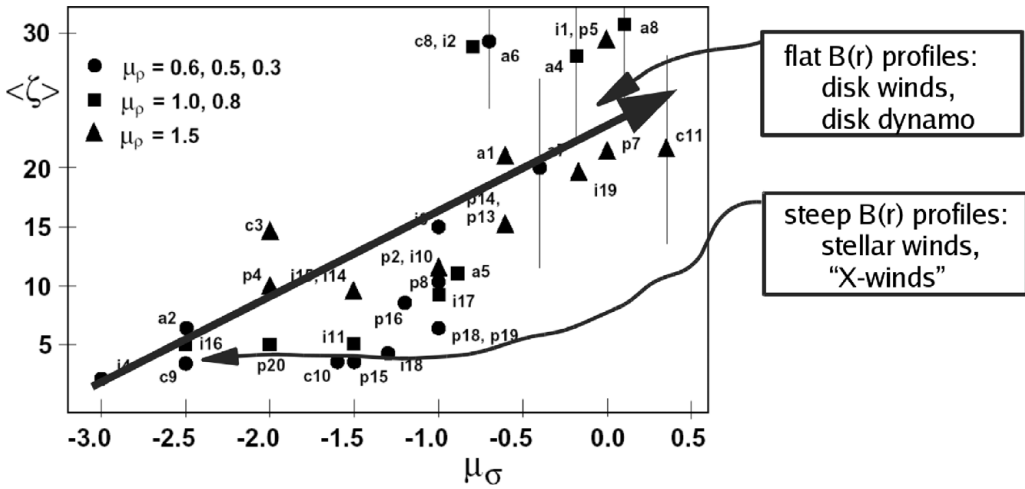


Figure 2. Collimation degree as function of the disk wind magnetic field, resp. magnetization profile. Error bars indicate flows which have not reached a steady state.

probably due to the success of MHD disk-jet models (Blandford & Payne (1982), Pudritz & Norman (1983)) - in particular for extragalactic jets - and the limitations of the early numerical simulations, this concept was somewhat repressed until it became evident that the young star itself does carry a substantial large-scale magnetic field.

For the numerical simulations of jet formation in general two approaches were made (see Fig.1). One is to prescribe the accretion disk properties as a boundary condition for the jet. Studying the acceleration and collimation of a disk/stellar wind requires essentially to follow the jet dynamical evolution for i) very long time ii) on a sufficiently large grid with iii) appropriate resolution. For such a goal, this second approach is better suited (Ustyugova *et al.* (1995), Ouyed & Pudritz (1997), Krasnopolsky *et al.* (1999), Fendt & Čemeljić (2002), Fendt (2006), Fendt (2009), Porth & Fendt (2010)). Naturally, the mass flux from disk to jet cannot be determined by such an approach. The other approach includes the disk structure in the simulation, in particular investigating the launching mechanism which lifts matter from the disk into the outflow, determining the mass flux from disk to jet (Uchida & Shibata (1984), Miller & Stone (1997), Goodson *et al.* (1997), Casse & Keppens (2002), Romanova *et al.* (2002), von Rekowski & Brandenburg (2004), Meliani *et al.* (2007), Zanni *et al.* (2007)). This approach is computationally expensive and still somewhat limited by spatial and time resolution. Thus, in many simulations published so far, the disk model underlying the jet launching is rather simple.

3. MHD simulations: disk jets with of different magnetic flux profiles

Here we present jet formation simulations where jets are formed from pure disk winds (see Fendt (2006)). The physical grid size corresponds to $(r \times z) = (150 \times 300) r_{in}$.

We start from a force-free initial field distribution in a hydrostatic equilibrium gas. The simulation evolves under the boundary condition of a (spatially and temporarily) fixed mass flux from the disk surface into the outflow. We run models covering a wide range of disk magnetic flux profiles and disk wind mass flux profiles, typically parameterized by power laws, $B_{p,wind}(r) \sim r^{-\mu}$, $\rho_{wind}(r) \sim r^{-\mu\rho}$. Both quantities can be combined in the disk wind magnetization parameter (Michel (1969)), $\sigma_{wind} \sim B_p^2 r^4 \Omega_F^2 / \dot{M}_{wind} \sim r^{\mu\sigma}$.

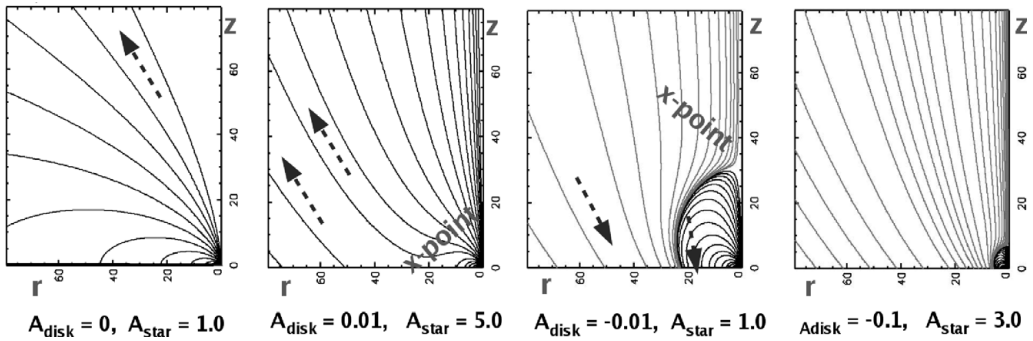


Figure 3. Initial magnetic field distribution for star-disk jet formation simulations, shown are poloidal magnetic field lines. Arrows indicate the magnetic field direction. Note the different location of the X-points. Different strength and orientation of the superposed stellar and disk magnetic field component, $A_{\text{disk}} = 0.0, 0.01, -0.01, -0.1$, resp. $A_{\text{star}} = 1.0, 5.0, 1.0, 3.0$ (from left to right). Note that here we show the left hemisphere (rotation axis directs upwards).

We quantify the collimation degree by comparing the axial and lateral mass fluxes (see Fendt & Ćemeljić (2002), Fendt (2006)). Figure 2) shows the collimation degree $\zeta \simeq (\dot{M}_z/\dot{M}_r)$ plotted against the power law exponent of the magnetization μ_σ . The main result is that steep magnetization profiles (e.g. the X-wind), resp. disk magnetic field profiles, are unlikely to generate highly collimated outflows. Flat profiles - generally leading to a higher collimation - tend to be unstable, i.e. do not establish a steady state.

4. MHD simulations: outflows from disk-star magnetospheres

We now discuss simulations considering the co-evolution of a stellar magnetosphere with a disk magnetic field. Both components are fed by a mass flux injected from the underlying physical boundary - the stellar surface and the accretion disk. We have used the ZEUS-3D codes extended for magnetic diffusivity (Stone & Norman (1992), Fendt & Ćemeljić (2002)). The field direction of both components can be aligned or anti-aligned. Similar configurations were considered early by Uchida & Low (1981).

Applying cylindrical coordinates (r, ϕ, z) , we divide the equatorial plane in three parts - the stellar surface $r < r_\star = 0.5r_{\text{in}}$, the disk $r > r_{\text{in}} = 1.0$, and the gap between star and disk. The stellar magnetospheric co-rotation radius is at the disk inner radius. The grid size is $(r \times z) = (80 \times 80)$ inner disk radii which refers to different physical scales when applied to e.g. protostars or XRBs. The initial (force-free) magnetic field is composed of a stellar (dipolar) field and a disk field (see Fig. 3),

$$\Psi_{\text{total}}(r, z) = A_{\text{disk}}f_{\text{disk}}(r, z) + A_{\text{star}}f_{\text{star}}(r, z), \quad (4.1)$$

where $\Psi_{0,\text{disk}}$ and $\Psi_{0,\text{star}}$ measure the strength of both components and the functions $f(r, z)$ describe the initial field distribution (see Fendt (2009)).

Figure 4 shows how the outflow evolves for the example with $\Psi_{0,\text{disk}} = -0.1$ and $\Psi_{0,\text{star}} = 3.0$. In this case, disk and stellar magnetic field direction (along the equatorial plane) are aligned. We evolve this simulation for 2800 rotations at the inner disk radius. At intermediate times (700 rotations) a quasi-stationary state emerges. One clearly sees the de-collimating effect of the central stellar wind component. Such quasi-stationary states may appear again on much longer time scales. We observe a cyclic behavior of the outflow opening angle with a periodicity of about 500 rotations.

Independent of the alignment, the central dipole does not survive on the large scale. A two-component outflow emerges: a stellar wind surrounded by a disk wind. For a

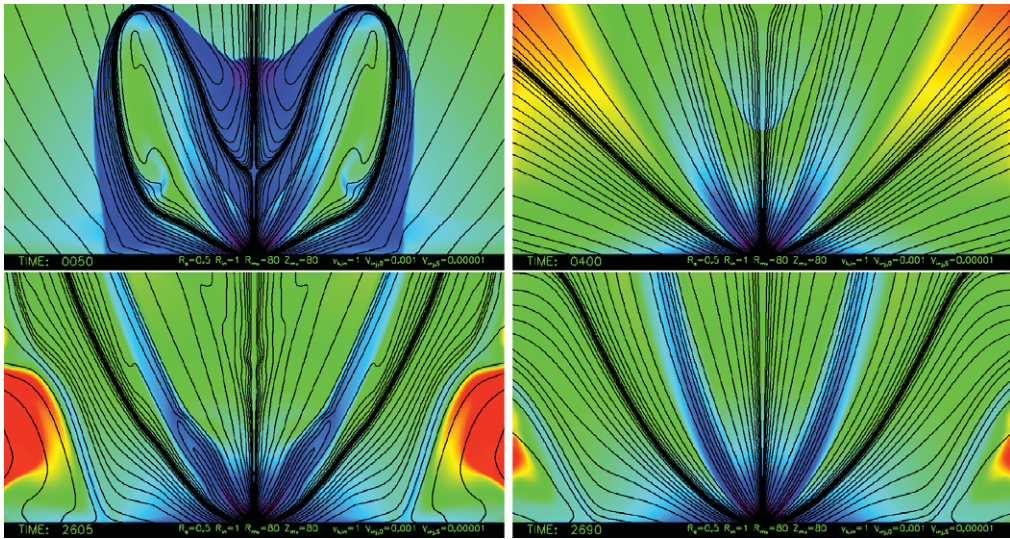


Figure 4. Time evolution of a star-disk magnetosphere from initial state of Fig. 3, middle. Time step is 50, 400, 2606, 2700 rotations of the inner disk (from top left to bottom right). Colors show logarithmic density contours, black lines are poloidal field lines (magnetic flux contours). Note that here we show both upper hemispheres (rotation axis directs upwards).

reasonably strong disk magnetic flux a collimated outflow emerges. If the overall flow is dominated by the stellar outflow, the disk wind remains un-collimated. Thus, the favorable setup to launch collimated jets from a star-disk magnetosphere is that of a heavy disk wind with strong magnetic flux.

We also observe reconnection events emerging from the X-point between the remaining inner dipole and the disk magnetic field, leading to sudden large-scale flares (see also Goodson *et al.* (1999)). The flare expansion is rapid and within few rotational periods. The flare events are accompanied by a temporal change in the outflow mass flux. Figure 5 shows the mass loss rate in axial direction integrated across the jet. We see two flares with a 20%-increase in the mass flux followed by a sudden decrease of mass flux by a factor of two. This behavior is also seen in the poloidal velocity profile.

Considering the ejection of large-scale flares and the follow-up re-configuration of outflow dynamics, we hypothesize that the origin of jet knots is triggered by such flaring events. Our time-scale for flare generation is of 1000 rotational periods and longer than the typical dynamical time at the jet base, but similar to the observed knots in protostellar jets. The flare itself for about 30-40 inner disk rotation times (see Fendt (2009) for a comparison to the Sweet-Parker reconnection time scale which turns out to be of the same order for the simulation parameters applied).

5. Jets from massive young stars

For massive young stars, the outflow dynamics is affected by the strong radiation field. Both the central object and the surrounding inner hot accretion disk may contribute to the radiative forces. Therefore, outflows from massive stars need to be modeled considering radiative forces and MHD. Vaidya *et al.* (2009) have shown that the inner disk can be internally heated up to 10^5 K while being sufficiently stable to launch an outflow.

Using the PLUTO code (Mignone *et al.* (2007)) we have run MHD simulations of jet formation under the influence of radiative forces from stellar and disk luminosity. The

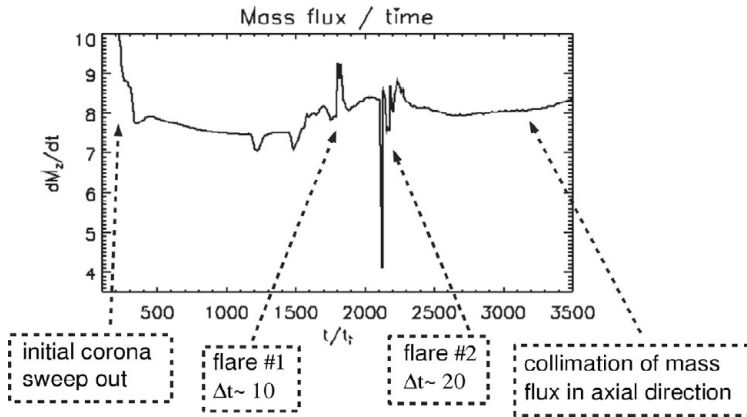


Figure 5. Time evolution of the axial mass flux close to the upper boundary. The mass flux changes during the initial evolution (sweep-out of the initial corona), but also during the flaring events.

radiative force $\mathbf{F}^{\text{rad}} = \mathbf{f}_{\text{cont},*} + \mathbf{f}_{\text{cont,disk}} + \mathbf{f}_{\text{line},*} + \mathbf{f}_{\text{line,disk}}$ considered in our study comprises of accelerations due to continuum radiation from star ($\mathbf{f}_{\text{cont},*}$) and disk ($\mathbf{f}_{\text{cont,disk}}$) and those due to lines forces from disk ($\mathbf{f}_{\text{line,disk}}$) and star ($\mathbf{f}_{\text{line},*}$). For the line forces we apply the well known CAK theory by Castor *et al.* (1975). This approach has been also explored for AGN disk winds by Proga (2003). The line force can be expressed as a product of force due to continuum radiation and a force multiplier $M(t)$, summarized over all lines, where t is the optical depth parameter. The parameter t is related to gradient of velocity along the l.o.s., the wind density, and the ion thermal speed v_{th} , thus $t = (\rho \sigma_e v_{th}) / |\hat{\mathbf{n}} \cdot \nabla(\hat{\mathbf{n}} \cdot \mathbf{v})|$.

An empirical form for $M(t)$ as a sum over all lines for model atmospheres for massive OB stars has been defined as $M(t) \sim kt^{-\alpha}$, where k and α are line force parameters Abbott(1982). Depending on the selection of lines, typical values obtained for k range from 0.4-0.6 and for α between 0.3-0.7. A force multiplier parameterization independent of arbitrary v_{th} , was introduced by Gayley(1995). The parameter \bar{Q} is related to parameter k initially introduced by Castor *et al.* (1975) as

$$M(t) = \left[\frac{\bar{Q}^{1-\alpha}}{1-\alpha} \left(\frac{|\hat{\mathbf{n}} \cdot \nabla(\hat{\mathbf{n}} \cdot \mathbf{v})|}{\sigma_e c \rho} \right)^\alpha \right] \quad (5.1)$$

Figure 6 show preliminary results (Vaidya & Fendt 2010, to be submitted). We start off with a pure MHD simulation similar to Ouyed & Pudritz (1997) or Fendt (2006). When a steady outflow is established (200 inner orbital periods), we switch-on the radiative forces (here only stellar line forces are considered). The radiative forces disturb the pure MHD jet structure, and a new quasi-steady state is reached after another 200 rotations.

The degree of collimation of the MHD jet under stellar radiation is higher. This is surprising, as one would naturally expect a *de-collimation* by the central flux. Our preliminary interpretation is that the stellar flux heats the lower (and inner) disk wind, by that changes the disk inflow boundary condition, resulting in an enhanced jet mass flux (by 20%). The higher mass load (and thus the larger outflow inertia) leads to a stronger toroidal field and a higher degree of collimation.

6. Relativistic MHD jet formation

We extended the previous non-relativistic simulations to the (special) relativistic regime. (Newtonian) gravity was added to enable a realistic Keplerian disk boundary

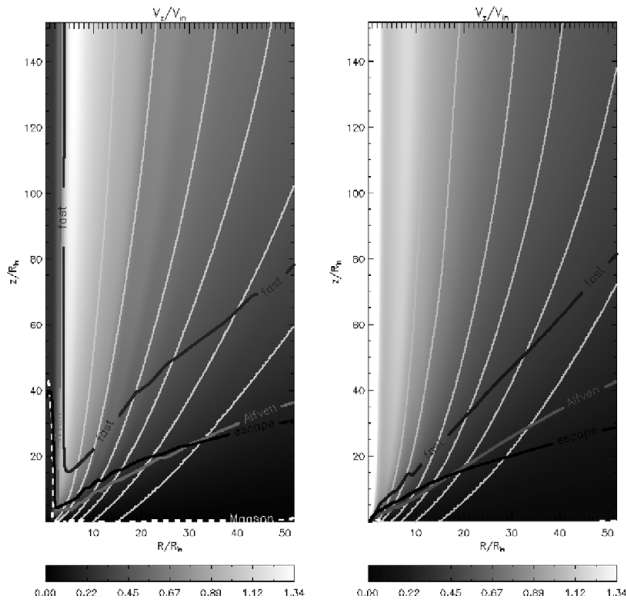


Figure 6. Jet formation simulations for massive young stars considering radiative forces. Pure MHD simulation for 200 disk periods (left), followed by a simulation including the stellar radiative force up to 400 disk periods (right). Mass fluxes are $\dot{M}_{\text{out}} = 2.7 \times 10^{-4} M_{\odot}/\text{yr}$ (left), and $\dot{M}_{\text{out}} = 3.9 \times 10^{-4} M_{\odot}/\text{yr}$ (right). The collimation degree derived from vertical/lateral mass fluxes is 0.86 (left), and 1.26 (right). The radiative forces is parametrized by the continuum flux force / gravity ratio $\Gamma_e = 0.14$, and the line force multiplier $Q_o = 2000$, $\alpha = 0.39$.

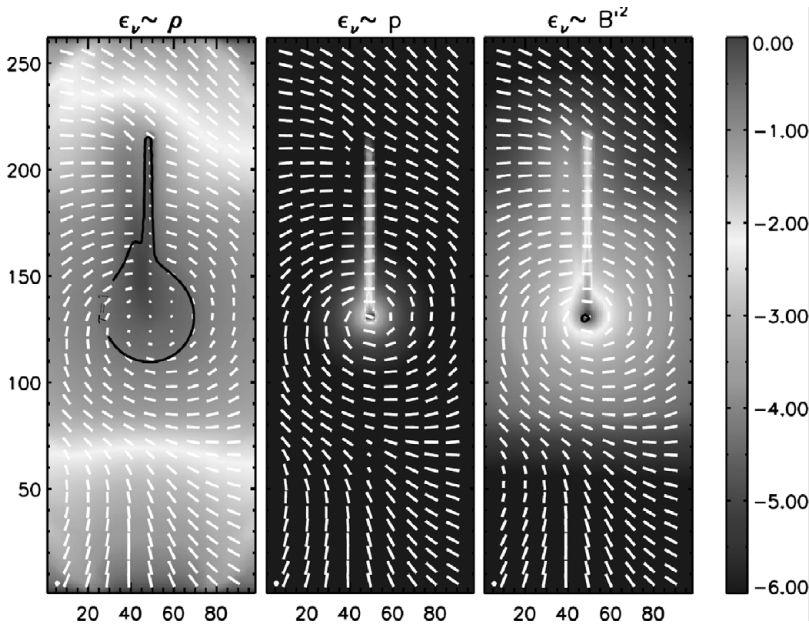


Figure 7. Ideal resolution synchrotron maps considering relativistic MHD simulations of jet formation and polarized radiation transfer. Results for three tracers for the particle acceleration are shown: density (left), thermal pressure (middle), magnetic energy (right). Shown are polarization vectors and the (normalized) 43 GHz intensity distribution for a viewing angle of 30 deg. The radial box size corresponds 400 inner disk radii.

condition for the jet (see Porth & Fendt (2010), and Fig.1, left). The resulting Lorentz factors of the jets reaches $\Gamma = 8 - 10$ depending on the Poynting flux injected.

The numerical results for the magnetohydrodynamic variable distribution were used to derive radio synchrotron maps following a relativistic polarized radiation transfer (Fig. 7). Since the particle acceleration is not included in the MHD model, additional assumptions have to be made. We applied three tracers for the power-law particle acceleration, ie. density, thermal pressure, or magnetic energy density (Porth & Fendt, submitted). All tracers give a similar polarization structure, although the intensity distribution differs. The spiky axial structure results from a high temperature, thin axial outflow from the compact object area and could be considered either as a Blandford-Znajek jet or a coronal wind.

References

- Abbott, D. C. 1982, *ApJ* 259, 282
 Blandford, R. D. & Payne, D. G. 1982, *MNRAS* 199, 883
 Casse, F. & Keppens, R. 2002, *ApJ* 581, 988
 Castor, J. I., Abbott, D. C., & Klein, R. I. 1975, *ApJournal*, 195, *ApJ* 195, 157
 Fendt, Ch. & Zinnecker, H. 1998, *A&A* 334, 750
 Fendt, Ch. & Ćemeljić, M. 2002, *A&A* 395, 1045
 Fendt, Ch. 2006, *ApJ* 651, 272
 Fendt, Ch. 2009, *ApJ* 692, 346
 Gayley, K. G. 1995, *ApJ* 454, 410
 Goodson, A. P., Winglee, R. M., & Böhm, K.-H. 1997, *ApJ* 489, 199
 Goodson, A. P., Böhm, K.-H., & Winglee, R. M. 1999, *ApJ* 524, 142
 Hayashi, M. R., Shibata, K., & Matsumoto, R. 1996, *ApJ* 468, L37
 Hirose, S., Uchida, Y., Shibata, K., & Matsumoto, R. 1997, *PASJ* 49, 193
 Krasnopolsky, R., Li, Z.-Y., & Blandford, R. D. 1999, *ApJ* 526, 631
 Meliani, Z., Casse, F., & Sauty, C. 2007, *A&A* 460, 1
 Michel, F. C. 1969, *ApJ* 158, 727
 Mignone, A., Bodo, G., Massaglia, S., Matsakos, T., Tesileanu, O., Zanni, C., & Ferrari, A. 2007, *ApJS* 170, 228
 Miller, K. A. & Stone, J. M. 1997, *ApJ* 489, 890
 Ouyed, R. & Pudritz, R. E. 1997, *ApJ* 482, 712
 Porth, O. & Fendt, C. 2010, *ApJ*, 709, 1100
 Proga, D. 2003, *ApJ*, 585, 406
 Pudritz, R. E. & Norman, C. A. 1983, *ApJ* 274, 677
 Pudritz, R. E., Ouyed, R., Fendt, Ch., & Brandenburg, A. 2007, in: B. Reipurth, D. Jewitt, & K. Keil (eds.), *Protostars & Planets V*, University of Arizona Press, Tucson, 2007, p.277
 von Rekowski, B. & Brandenburg, A. 2004, *A&A* 420, 17
 Romanova, M., Ustyugova, G., Koldoba, A., & Lovelace, R. 2002, *ApJ* 578, 420
 Stone, J. M. & Norman, M. L. 1992, *ApJS* 80, 753
 Shang, H., Li, Z.-Y., & Hirano, N. 2007, in: B. Reipurth, D. Jewitt, & K. Keil (eds.), *Protostars & Planets V*, University of Arizona Press, Tucson, 2007, p.261
 Uchida, Y. & Low, B. C. 1981, *Journal of Astroph. and Astron.* 2, 405
 Uchida, Y. & Shibata, K. 1984, *PASJ* 36, 105
 Uchida, Y. & Shibata, K. 1985, *PASJ* 37, 515
 Ustyugova, G., Koldoba, A., Romanova, M., Chechetkin, V., & Lovelace, R. 1995, *ApJ* 439, 39
 Vaidya, B., Fendt, C., & Beuther, H. 2009, *ApJ* 702, 567
 Zanni, C., Ferrari, A., Rosner, R., Bodo, G., & Massaglia, S. 2007, *A&A* 469, 811

Discussion

FALCKE: Does the radiation pressure (from the disk) potentially also play a role in AGN jets?

FENDT: I would guess so. We intend to apply the model also to AGN jets. Disk radiation forces will, however, mainly accelerate the material. But MHD will dominate. Second order effects could be an enhanced mass flux compared to pure MHD jets.